SCIENTIFIC REPORTS

OPEN

Duality picture of Superconductor-insulator transitions on Superconducting nanowire

Received: 11 February 2016
Accepted: 10 May 2016
Published: 17 June 2016

Kazumasa Makise[1], Hirotaka Terai[1], Yukihiro Tominari[1], Shukichi Tanaka[1] & Bunju Shinozaki[2]

In this study, we investigated the electrical transport properties of niobium titanium nitride (NbTiN) nanowire with four-terminal geometries to clarify the superconducting phase slip phenomena and superconducting-insulator transitions (SIT) for one-dimensional superconductors. We fabricated various nanowires with different widths and lengths from epitaxial NbTiN films using the electron beam lithography method. The temperature dependence of resistance $R(T)$ below the superconducting transition temperature T_c was analyzed using thermal activation phase slip (TAPS) and quantum phase slip (QPS) theories. Although the accuracy of experimental data at low temperatures can deviate when using the TAPS model, the QPS model thoroughly represents the $R(T)$ characteristic with resistive tail at low temperatures. From the analyses of data on T_c, we found that NbTiN nanowires exhibit SIT because of the change in the ratio of kinetic inductance energy and QPS amplitude energy with respect to the flux-charge duality theory.

The state-of-the-art superconducting quantum computer consists of superconductor-insulator-superconductor tunnel junctions called Josephson junctions because it is a commonly used for superconducting digital circuits and quantum qubit for quantum computing devices. Recently, one-dimensional (1D) superconducting nanowires (SNWs) are being considered to develop superconducting computing devices[1,2]. In order to realize novel devices using nanowires, it is necessary to clarify the superconducting transport characteristics that depend on the disorder, wire length L, width w, and many other parameters. In such low-dimensional superconductors, quantum effects slightly influence the superconducting characteristics. For instance, on when the film thickness d of the two-dimensional (2D) specimens decreases, the superconducting transition temperature T_c is gradually depressed and then the superconductivity disappears for films thinner than the critical thickness d_c, where the 2D superconductor-Insulator transitions (SIT) occurs[3–6]. T_c depression is expected by enhanced Coulomb repulsion due to increase of disorder[7]. As for other tuning parameters of SIT, we can consider not only the film thickness but also the external magnetic field and carrier density[8]. The SIT originates from the fluctuations of an amplitude and/or a phase of superconducting order parameter. Especially, SNWs can be strongly affected by thermally activated phase slip (TAPS)[9,10] and/or quantum phase slips(QPS)[11,12] which play an important role in the properties of SNWs. The effect of TAPS to resistance $R(\Omega)$ sharply decays as a result of the temperature drop below T_c. On the other hand, the QPS represents the residual resistance required to suppress the superconductivity at $T = 0$ K. Numerous studies have been conducted on the various materials that can be used for SNWs[13–18]. However, there still are fundamental problems in determining the effect of TAPS and QPS on the temperature dependency of resistance $R(T)$ because SNW specimens with the same material can present different $R(T)$ characteristics. Further, some investigations show no evidence of QPS behavior at very low temperatures[14,17,18].

Another attractive subject of investigation for SNWs is clarifying some critical values corresponding to SIT, namely, the normal state critical resistance R^N_c, $(R^N/L)_c$, or other characteristics. Several research groups have reported the characteristics of $R(T)$ below T_c and SIT for MoGe SNWs[13,17,18]. For $(R^N/L)_c$, separating 1D specimens into superconducting and insulator phases, the $(R^N/L)_c$ takes the almost same values in the region $30 < (R^N/L)_c < 100$. On the other hand, $R(T)$ characteristics show different behaviors owing to the TAPS or QPS mechanisms. Although Marković *et al.*[19] and Tinkham *et al.*[13] observed broad transition with a resistive tail due to the QPS at low temperatures, others[14,17] fit the TAPS model to data without the resistive tail. As for R^N_c, it is expected to take the superconducting quantum resistance $R_Q = h/4e^2 \approx 6.45$ KΩ for Cooper pairs[20–22]. This

[1]National Institute of Information and Communications Technology, Kobe 651-2492, Japan. [2]Department of Physics, Kyushu University, Fukuoka 819-0395, Japan. Correspondence and requests for materials should be addressed to K.M. (email: makise@nict.go.jp)

suggestion is conformed for short wires by phenomenological model[23] and experimentally confirmed for specimens with a length of $L < 200$ nm[14]. However, the data for longer specimens are inconsistent in that they exhibit $R^{N}_{c} > R_Q$ and show superconductivity[15,24]. Thus, there is no consensus between experiments and theories on the exact role of SIT of 1D-SNWs.

Recently, Mooij *et al.* proposed an idea that the concept of flux-charge duality can relate the QPS with Josephson tunneling if the roles of phase and charge are interchanged[1]. They discussed the crossover value between superconducting and insulating states at low temperatures as a function of ratio $\alpha = E_s/E_L$, where E_s and E_L are the QPS energy and inductive energy, respectively. Increasing E_s leads to a transition from inductively superconducting regime where $E_L \gg E_s$ to a capacitive insulating regime where $E_s \gg E_L$. Further, they succeeded in showing the phase boundary between the superconducting and insulating state of data for MoGe SNWs[14] by assuming $\alpha = 0.3$.

To observe the quantum phase slip in SNWs, specimens are required to be homogeneous and satisfy the condition $d,w \le \xi$, where ξ is superconducting coherence length. Further, poor links due to inhomogeneities in the superconducting wires can cause residual resistance at low temperatures as pointed by Altomare *et al.*[15] In the present report on homogenous nanowires, the $R(T)$ characteristics of NbTiN SNWs in a broad range of the R^N/L were investigated from the viewpoint of QPS mechanisms. We analyzed the data from the superconducting and insulating phase diagrams based on the flux-charge duality model using the relation $(R^N/R_Q)/(L/\xi)$ versus L/ξ with a suitable parameter α and other parameters in theories[1].

Experimental Procedure

Superconducting NbTiN films were firstly prepared by deposition at ambient temperatures on (100)-MgO substrates by DC reactive magnetron sputtering. The background pressure of the chamber was maintained below 2.0×10^{-5} Pa. The relative amounts of argon and nitrogen were controlled by mass flow controller during sputtering. The total pressure was maintained at 2 mm torr and the substrate was not heated intentionally during deposition. Details of preparation procedures and films quality of NbTiN thin films are previously reported[25]. The NbTiN SNWs were fabricated from 2D films with $d = 5$ nm by a conventional e-beam lithography method and a reactive ion etching method with CF_4 plasma. The ranges of L and w of nanowires are $250 \le L \le 1000$ nm and $10 \le w \le 30$ nm, respectively. To eliminate the influence of the contact resistance, measurements of transport properties were performed by four-probe method. The normal state resistance, R^N, is defined as the sample resistance at 20 K. The T_C and H_{C2} were defined as the point at which the R^N reached half its value.

Results and Discussion

Figure 1(a) shows the scanning electron microscopy image of typical NbTiN SNWs. Figure 1(b) presents the characteristics of $R(T)$ for various SNWs with different values of w and L. Superconducting SNWs that have $dR/dT > 0$ under low temperatures and low $R(\Omega)$ characteristics, experience the initial drop of $R(\Omega)$ almost at the same temperature owing to the superconducting transition. An increase in R^N causes T_c and the residual resistance to monotonically decrease and increase, respectively. Prior to the detailed discussions on the SIT of 1D specimen from a viewpoint of quantum phase transition, we will present some transport properties of the present SNWs from the characteristics of low dimensional superconductors.

Figure 2(a) shows a typical $R(T)$ of the NbTiN SNWs with $L = 500$ nm and $w = 20$ nm at various external magnetic fields. With an increase in H, T_c monotonically decreases without field-tuned SIT even at $H = 9$ T. On the other hand, as shown in the inset, the 2D NbTiN with almost the same thickness (≈ 5 nm) shows that the field-tuned SIT occurs around 5–6 T where many vortexes in the film appear to transition into super-fluid states of vortexes in the dirty boson scenario[26–28]. The present result for NbTiN SNWs suggests that this nucleation of the vortex in the superconducting state is inhabited because of the 1D-restricted geometry of the nanowire. We consider the dimensionality and size effects of the nanowire on the upper critical magnetic field H_{c2}. The suppression of superconductivity by perturbations is given by the relation, $\ln[T_c(H)/T_c(0)] = \Psi(1/2) - \Psi[1/2 + \delta/2\pi k_B T_c(H)]$, where $\Psi(x)$ is the digamma function and δ is the pair-breaking strength which depends on the dimensionality of the specimen and the direction of the external magnetic field[29]. Expanding the function $\Psi[1/2 + \delta/2\pi k_B T_c(H)]$ around $x = 1/2$, we obtained the relation $k_B[T_c(0) - T_c(H)] = \delta\pi/4$in the temperature range near $T_c(0)$, where δ is given by $\delta = DeH/c$ and $\delta = DeH^2d^2/6\hbar c^2$ for fields perpendicular and parallel to the surface of 2D specimen with $d < \xi(0)$, respectively, and D is the diffusion constant. From the above relation, $H_{c2}(T)$ near $T_c(0) \equiv T_{c0}$ is given by

$$H_{c2}(T) \propto (1 - T/T_{c0})^n, \quad (1)$$

where the index n is 1 and 1/2 for magnetic fields perpendicular and parallel to the surface, respectively. When the expression for the parallel case is approximately applied to SNWs, it is expected that n approaches 1/2 with $w \approx \xi(0)$. By using the Eq. (1), we obtained the index n for each SNW. Figure 2(b) shows the R/L dependence of n for NbTiN SNWs, where the dotted line is the reference point. It can be seen that the index n approaches 0.5 with an increase in the R/L ratio. The inset shows the typical data of $H_{c2}(T)$ for the SNW with $w = 10$ nm and $L = 500$ nm. The solid line shows Eq. (1) with $n = 0.56$. These results indicate the 1D transport property of the present SNWs.

To clarify the mechanism of the resistive tail for NbTiN SNWs at low temperatures shown in Fig. 1(b), we analyzed the $R(T)$ and the voltage-current characteristics in a broad temperature range. The fluctuation of the superconducting order parameter $\psi(r)$ plays an important role in the transport properties of the 1D superconductor. The magnitude of $\psi(r)$ vanishes at some points in the SNWs owing to the fluctuation, and it recovers the phase slip by 2π. There are two mechanisms for the phase slip, TAPS and QPS. According to the TAPS model, dV/dI and $R_{TAPS}(T)$ are expressed by[9,10]

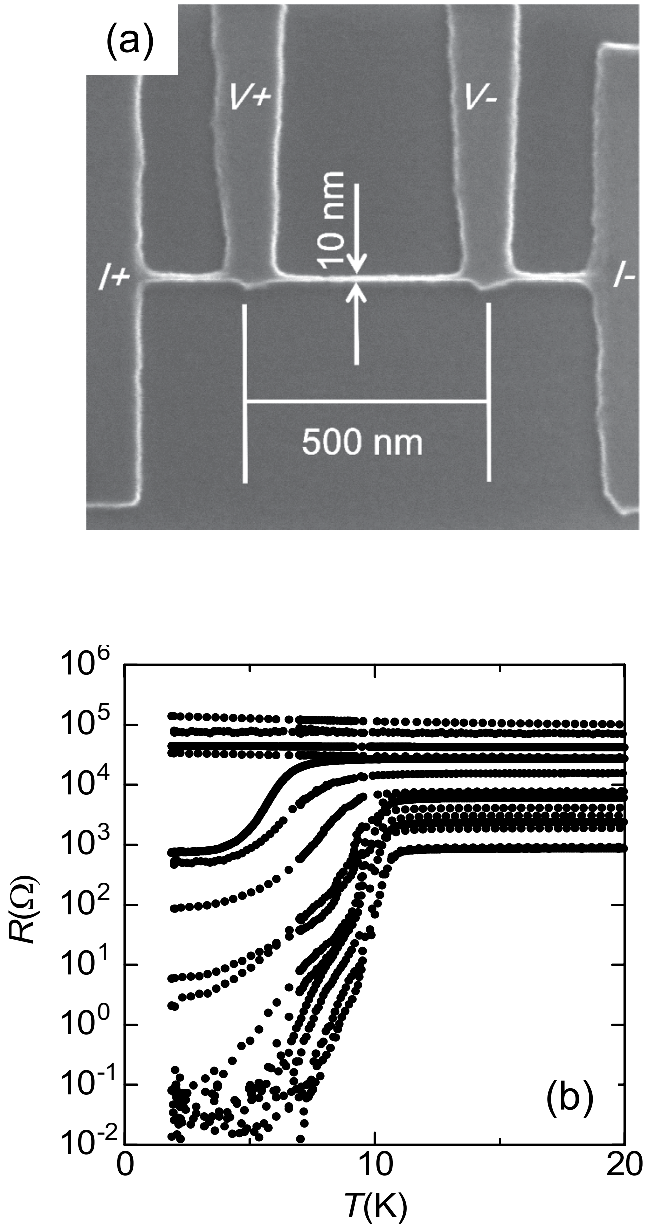

Figure 1. (**a**) Scanning electron microscopy image of a NbTiN SNW with 10 nm-width. (**b**) $R(T)$ for in series of NbTiN SNWs within ranges of 250–1000 nm length L and 10–30 nm width w.

$$dV/dI = (\hbar\Omega/4e^2k_BT)\exp[-\Delta F(T)/k_BT]\cosh(I/I_0), \tag{2}$$

and

$$R_{TAPS} = (dV/dI)_{I\rightarrow 0} = (\hbar\Omega/4e^2k_BT)\exp[-\Delta F(T)/k_BT] \tag{3}$$

where $\Omega = (L/\xi)(\Delta F/k_BT)^{1/2}(1/\tau_{GL})$, $\Delta F(T) = 0.83k_BT_c(R_Q/R^N)(L/\xi(0)(1-T/T_c)^{3/2}$ is the energy barrier, $I_{0,TAPS} = (4ek_B/h)T$ and $\tau_{GL} = [\pi\hbar/8k_B(T_c - T)]$ is the relaxation time of G-L equation. On the other hand, $R_{QPS}(T)$ is expressed as

$$R_{QPS}(T) = \beta R_Q S_{GZ}\frac{L}{\xi(T)}e^{-S_{GZ}} \tag{4}$$

where $S_{GZ} = \eta\frac{R_Q}{R_N}\frac{L}{\xi(T)}$ is the normalized unit measured by R_Q and $\xi(T)$, and β and η are fitting parameters held constant on the order of unity[30,31]. For $\xi(T)$, the expression $\xi(T) = 0.907\xi(0)\left(1 + (1 - 0.25t)\frac{\xi(0)}{t}\right)^{-1/2}(1 - t^2)^{-1/2}$ is adopted[32]. The dV/dI is also given by

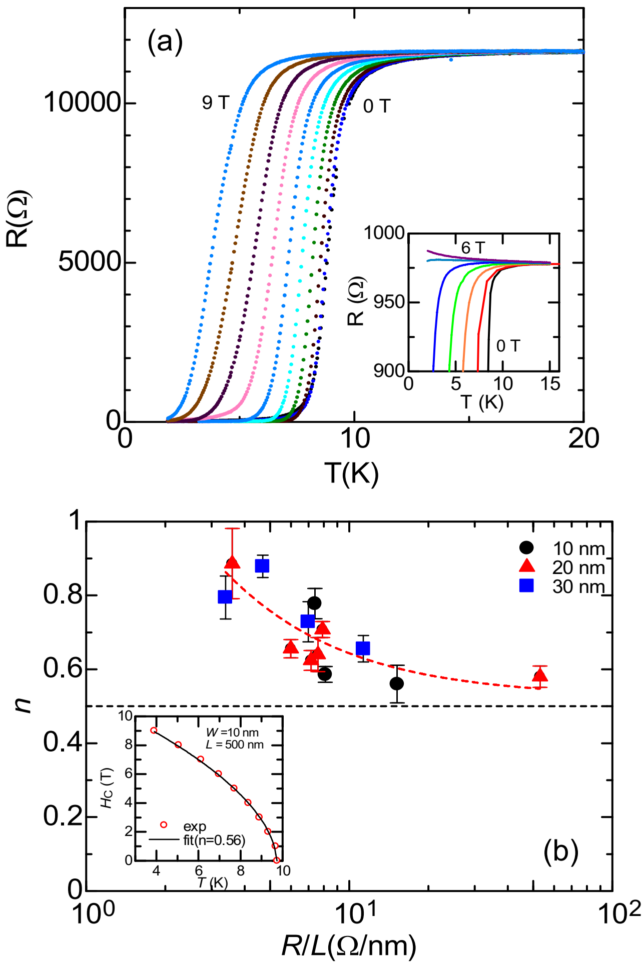

Figure 2. (**a**) $R(T)$ for the NbTiN SNW with $d = 5$ nm, $w = 20$ nm and $L = 500$ nm under the magnetic field ranging from 0 to 9 Tesla with a division of 1 Tesla. Inset shows the $R(T)$ for the NbTiN film with the same thickness of the nanowire under the magnetic field. (**b**) R^N/L dependence of the index n in Eq. (1). Inset shows the typical $H_{c2}(T)$ for the nanowire with $w = 10$ nm. Where the solid line is represented by calculating Eq. (1).

$$dV/dI = R_{QPS}(T)\cosh(I/I_{0,QPS}), \tag{5}$$

where $I_{0,QPS}$ is expected to have a different temperature dependence from $I_{0,TAPS} = (4ek_B/h)T$.

Figure 3 shows the superconducting transport properties for the NbTiN SNW with $d = 5$ nm, $w = 10$ nm, $L = 500$ nm, $T_c = 10.0$ K, and $R^N = 5.0$ kΩ. Figure 3(a) shows $R(T)$ from the measurements of current-bias (○), and the dV/dI (■) at $I \approx 0$ shown in Fig. 3(b). The calculation made using the TAPS model shown by the dashed line (---) cannot explain $R(T)$ characteristic except for temperatures close T_c and unfortunately, the theory strongly deviates from the data below 8 K. This discrepancy suggests that transport properties of the present NbTiN SNWs are incompatible with TAPS theory at low temperatures. The solid line is calculated using Eq. (4) with parameters of $\xi(0) = 8$ nm, $\beta = 0.0013$, and $\eta = 0.024$ in order to fit theory with $R(T)$ data under a broad temperature range. The calculation using the QPS model agrees accurately with the resistive tail in the range of 5 magnitude orders. Figure 3(b) represents the I–V characteristics at temperatures of 2 K, 5 K, 6 K, 7 K, 8 K, and 9 K. The I–V curves have shown nonlinear characteristic in the superconducting region below the 9 K. This I dependence of dV/dI at each temperature agrees well with the term of $\cosh(I/I_{0,QPS})$ in the Eq. (5) as shown by the solid lines[33]. From the fitting procedure, we obtained the temperature dependences of R and $I_{0,QPS}$. The inset in Fig. 3(b) shows the $I_{0,QPS}(T)$, which is almost independent of temperature as shown by the dotted line. This discrepancy with the TAPS model shown by the solid line is consistent with the experimental result that $R(T)$ cannot be explained by the TAPS model.

Before investigating the R^N/L ratio dependence on T_c in order to clarify the SIT of NbTiN SNWs, we will analyze the data using the theory based on the dynamically enhanced Coulomb repulsion competing the attractive interactions between electrons[7]. The theoretical expression for T_c is given by a simple formula as a function of sheet resistance R_{sq} (resistance for unit area) with the parameter $\gamma = 1/\ln(k_B T_{c0}\tau/1.14\hbar)$, where τ is the electron elastic scattering time. Figure 4 represents the R_{sq} dependence of T_c for both nanowire specimens and 2D specimens. T_{co} values are expected to be independent of w and L as shown in Fig. 5, because the T_c on the vertical axis is normalized by $T_{c0} = 11.0$ K of pure 2D films. Although R_{sq} of 2D specimens was controlled by changing the

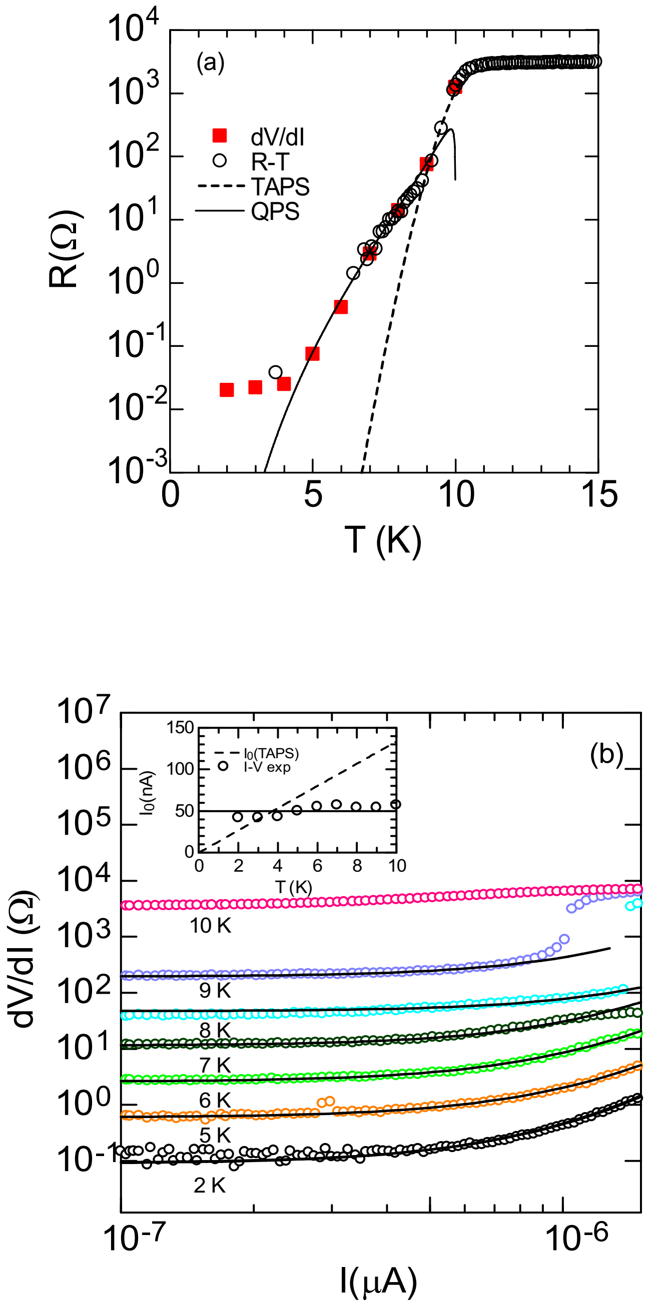

Figure 3. (**a**) $R(T)$ for the NbTiN SNW with $d = 5$ nm, $w = 10$ nm and $L = 500$ nm. Open circles are resistances from the low bias current measurement and squares show resistances obtained by applying the theory to the data of dV/dI in (**b**). Dotted and solid lines are calculated using Eq. (2) and Eq. (4), respectively. (**b**) Bias current dependence of differential resistance under various temperatures below T_c. Solid lines are calculated using Eq. (3). The inset shows the temperature dependency of $I_{0,QPS}$. The dashed line shows $I_0(T) = (4ek/h)T$ predicted by the TAPS theory. Solid line $I_0 =$ constant is a reference point.

thickness, R_{sq} of SNW specimens with different w was controlled by changing the length L and by keeping the thickness constant at $\approx 5\,nm$ for all SNWs. The dotted line is calculated by using the theory for impure 2D system[5] in order to fit the data ($\times$) with a parameter $\gamma = 1/\ln(k_B T_{C0}\tau/\hbar)$. The good agreement between the theory and data suggests that the T_c depression of 2D NbTiN films is determined by the decrease in the amplitude of the superconducting order parameter that belongs to the system confirming the fermionic scenario. As for 2D NbN and NbTiN films, we have already investigated transport properties on the fluctuations and SIT[5,28]. We reported that the critical sheet resistance R_c is approximately 2.2 kΩ and superconducting suppression mechanism can be explained by the localization theory. On the other hand, data for SNW specimens in the range of $10\,\text{nm} \le w \le 30\,\text{nm}$ do not collapse on the unique line calculated by the theory[7]. In addition, the depression of T_c cannot be explained only by enhanced Coulomb interaction in impure superconductors.

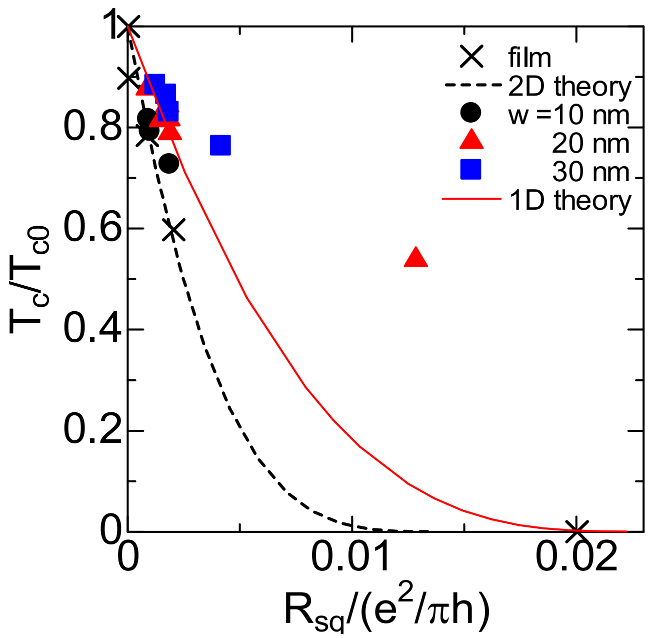

Figure 4. **R_{sq} dependence of T_c for NbTiN film and nanowire specimens.** Dotted and solid lines are calculated from theories based on the dynamically enhanced Coulomb repulsion in dirty systems for the film and nanowire, respectively.

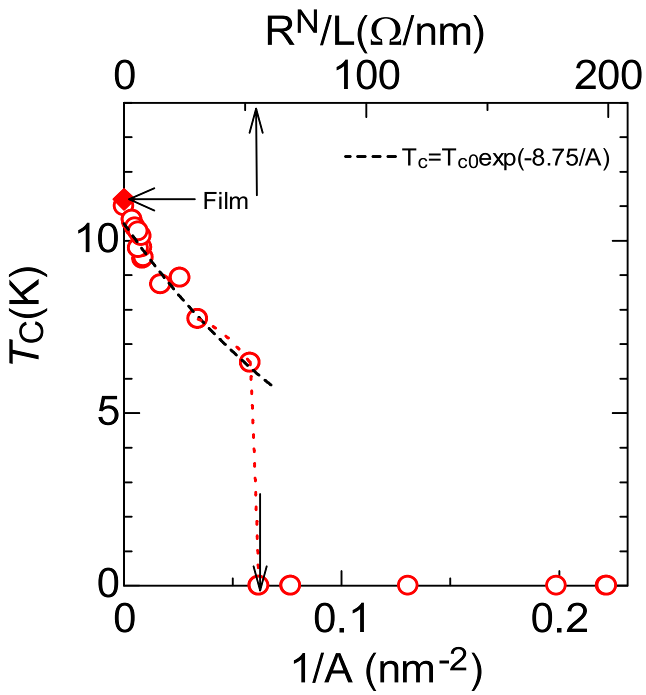

Figure 5. **R^N/L (upper horizontal axis) and 1/A (down horizontal axis) dependencies of T_c for NbTiN SNWs.** Mark (◆) represents the T_c for 2D specimens. The broken line represents $T_c = T_{c0}\exp(-8.75/A)$ determined from data. The dotted line is the reference point. Arrows, ↑ and ↓ indicate the SIT points.

Figure 5 shows T_c as functions of $[R(20\,\mathrm{K} > T_c) \equiv R^N]/L$ (upper axis) and $1/A$ (lower axis), where the cross section area A is derived from the relation $R^N/L = \rho/A$ using the resistivity value of $\rho = 0.9\,\mu\Omega\mathrm{m}$ determined before the fabrication of 2D films. The T_c was defined as the temperature at which the resistance takes one half of $R(20\,\mathrm{K})$. For specimens with different size of w and L, data of T_c concurs well onto a single curve in a broad R^N/L (or $1/A$) range. This fact expresses that the quantity R^N/L ratio is a sufficient parameter to describe the impurity

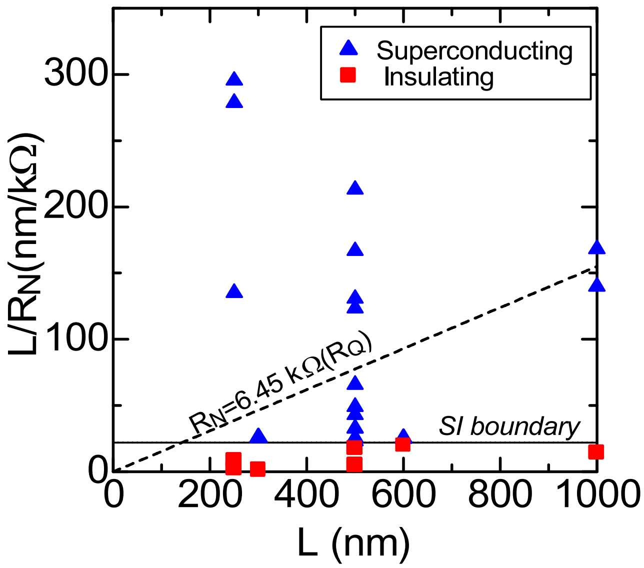

Figure 6. Phase diagram of R^N/L versus L for NbTiN SNWs. Squares (■) and triangles (▲) represent insulating and superconducting wires, respectively. The solid line indicates the boundary of SIT estimated from experimental results of R-T characteristics. The dotted line is the boundary of SIT expected from the Chakravarty-Schmid-Bulgadaev theory. (see text.).

dependence of T_c for the 1D system and for 2D system in the case R^N is replaced with R_{sq}. The T_c slowly decreases below the value $R^N/L \approx 50\Omega$/nm when R/L increases, and rapidly decreases in the range above 50–60 Ω/nm. For a relation between T_c and R^N/L in Fig. 5, Marković *et al.*[19] proposed a simple criterion for the crossover value of $(R^N/L)_{c.o}$ separating an insulating state from superconducting state. If the wire resistance at $T = 0$ due to the quantum phase slip is comparable to R^N, the resistance drop does not appear to sustain the value of R^N even at very low temperatures. Using Eq.(4) at $T = 0$, they obtained the normalized resistance due to quantum phase slips[24] as

$$R_{S\xi} = 2\pi \exp[-0.33/R_{N\xi}], \tag{6}$$

where the resistances $R_{S\xi}$ and conductance $R_{N\xi}$ are measured in units of quantum resistance R_Q and length in units of coherence length ξ, namely, $R_{S\xi} = (R_S/R_Q)/(\xi/L)$ and $R_{N\xi} = (R^N/R_Q)/(\xi/L)$. From Eq. (6), by equating $R_{S\xi}$ to the R^N, we obtain the value $(R^N/L)_{c.o} = R_Q/13.3\xi(0) \approx 485\Omega/\xi(0)$. As for the present series of which $\xi(0) \approx 9\,nm$, we obtain $(R^N/L)_{c.o} \approx 54\Omega$/nm. This value is almost the same one denoted by the arrow ↑ separating the superconductor and insulator phases in Fig. 5.

From $1/A$ dependence of T_c in Fig. 5, we can quantitatively discuss on the critical diameter D_c of NbTiN SNW at SIT. The dotted line in Fig. 4 represents the relation $T_c = T_{co} \exp(-u/A)$, where $T_{c0} = 11.0$ K and $u = 8.75\,nm^2$ are the transition temperature of 2D film and the parameter determined from the fitting procedure, respectively. $1/A$ dependency of T_c has also been reported in $Mo_{78}Ge_{22}$ and $Mo_{50}Ge_{50}$ SNWs[18] that is having greater α than that of the present NbTiN. If this relation for NbTiN SNW is valid for board range $1/A$, the $D_c \propto u^{1/2}$ value is expected to be smaller than ≈2 nm. On the other hand, the $T_c(1/A)$ characteristic drastically decreases around $1/A \approx 0.06\,nm^{-2}$, giving $D_c \approx (4A/\pi)^{1/2} \approx 4.6\,nm$ denoted by the arrow ↓, which is approximately half of the 2D NbTiN coherence length $\xi(0) \approx 9\,nm$ determined from the relation $\xi^2(0) = (\hbar c/2eT_c)|dT/dH_{c2}(T)|_{T\approx T_c}$[6]. This estimation suggests that the restricted geometry of SNW allows smaller critical diameter than $\xi(0)$ for 2D specimens.

Now, we will discuss of size dependence of T_c and SI phase diagram for the present SNWs. To clarify the 1D SIT mechanisms of NbTiN SNWs, we illustrated the SI phase diagram in Fig. 6 according to the Chakravarty–Schmid–Bulgadaev theory based on the interaction of QPS and dissipative environment[20–22]. Such a relation between L and L/R^N has been reported for MoGe SNWs[14]. The author claimed that the SIT boundary is given by a condition $R^N = R_Q = 6.45\,k\Omega$. However, the present NbTiN SNWs specimens with $L > 500\,nm$ do not satisfy this condition as shown by the dashed line, that is, specimens with $L > 500\,nm$ show superconductivity though R^N is larger than R_Q. Although the $R(T)$ characteristic of NbTiN SNWs can be explained by the QPS theory as discussed in Figs 4 and 5, the phase diagram shown in Fig. 6 suggests that the SI boundary depends on the length of the nanowire.

QPS and the Josephson effects in SNWs are related to each other by a concept of duality transformation. According to this concept[1], the SIT is determined by the ratio between the strength of QPS amplitude energy E_S and SNW inductive energy E_{Li}. Both energies are given by $E_S = eV_0/\pi = a(L/\xi)k_BT_c(R_Q/R_\xi)\exp(-bR_Q/R_\xi)$ and $E_{Li} = \phi_0/2L_i = 17.4k_BT_c(R_Q/R^N)$, where the $R_\xi = R^N\xi/L$ is the resistance of the SNW over an appropriate length, $L_i = 0.18\hbar R^N/k_BT_c$ is the kinetic inductance of the wire, $\Phi_0 = h/2e$ is the flux quantum, and a and b are constants of order one. According to Mooij *et al.*[1], it is expected that SIT occurs at condition $E_s/E_{Li} = (a\lambda^2/17.4)$

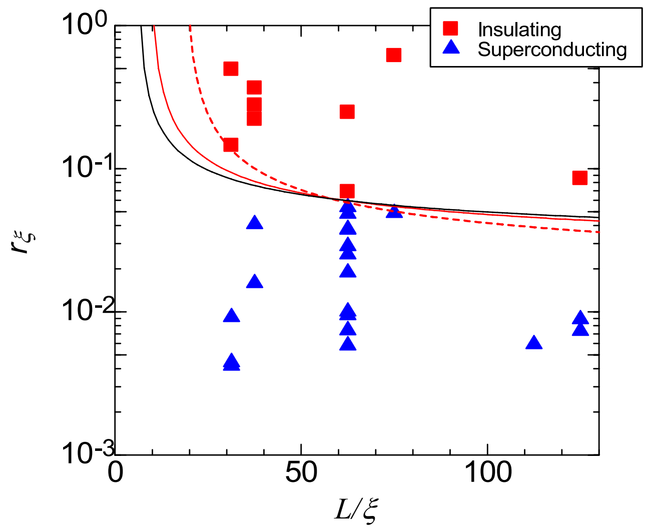

Figure 7. Phase diagram of $L/\xi(=\lambda)$ versus $r_\xi = (R^N/R_Q)/(L/\xi)$ for NbTiN SNWs. (■) and (▲) are the same marks in Fig. 6. Lines denoted by (---), (—) and (—) are calculated from Eq. (7) with input parameters $(b, c) = (0.14, 0.05)$, $(b, c) = (0.23, 0.2)$ and $(b, c) = (0.28, 0.5)$, respectively.

$\exp(-b/r_\xi) = \alpha_c$, where $\lambda = L/\xi_i$ and $r_\xi = R_\xi/R_Q (= R^N\xi/R_Q L)$ are the normalized length and resistance, respectively. From the equation for E_s/E_{Li}, we obtain the λ dependence of r_ξ as

$$r_\xi(\lambda) = b/\ln(a\lambda^2/17.4\alpha_c) \equiv b/\ln(c\lambda^2/17.4). \quad (7)$$

Figure 7 shows the $r_\xi(\lambda)$ for all same NbTiN SNWs shown in Fig. 6, where $\xi = 8$ nm is used. To show a boundary separating the superconducting phase from the insulator phases, we calculate $r_\xi(\lambda)$ from Eq. (7) with input parameters b and c. Although data are not so large to make clear the boundary, we attempt to find reasonable values for b and c assuming that the theoretical line must go through a reliable point of $r_\xi(\lambda) \approx 0.6$ at $\lambda(=L/\xi) \approx 62$ for analysis. The red-broken, red-solid, and black-solid lines are typically calculated from Eq. (7) to divide the data into superconducting and insulator phases with the use of parameters $(b, c) = (0.14, 0.05)$, $(b, c) = (0.23, 0.2)$ and $(b, c) = (0.28, 0.5)$, respectively. When we take into account the theoretical suggestions that the strength p of three parameters a, b and α_c is given as $0.1 < p < 1$. Further, the first combination of $(b, c) = (0.14, 0.05)$ corresponds to $(\alpha_c, a, b) = (0.025, 0.5, 0.14)$ due to the definition $c = a/\alpha_c$ in Eq. (4). This critical ratio $\alpha_c = 0.025$ is very small compared with the theoretical suggestion. On the other hand, other combinations shown by solid and dotted lines give reasonable values for a and b, namely, $0.1 < a < 0.25$ and $0.23 < b < 0.28$ for $\alpha_c = 0.5$. These values are comparable to those analyzed by Mooij *et al.* for Mo/Ge SNWs data.

Conclusion

We investigated the transport properties of superconducting NbTiN SNWs in a wide range of R^N/L using four-probe method to eliminate the contact resistance. The $R(T)$ characteristic with resistive tail below T_c for SNWs with high values of R^N/L can be well explained by the QPS theory. With the increasing R^N/L, the behavior of the $R(T)$ characteristic changes from superconducting to insulating. $R(T)$ exhibits superconducting-insulator transition near $(R^N/L)_{c.o} \approx 60\,\Omega$/nm, which agrees well with the prediction based on the QPS model by Marković *et al.* As for the S-I phase boundary for the NbTiN SNWs, the phase diagram L/R^N vs. L is inconsistent with Chakravarty–Schmid–Bulgadaev theory, which has succeeded in describing the SIT for short MoGe SNWs. On the other hand, the analysis based on the model for the SNW which is being dual element upto Josephson junction, suggests that the separation of the superconducting and insulator phases may be controlled by the ratio of QPS amplitude energy E_S and inductive energy of SNW E_{Li}, E_s/E_{Li}. For the present NbTiN series, we observed that SIT may occur at $0.2 < E_s/E_{Li} < 0.5$.

References

1. Mooij, J. E. & Narazov, Yu. V. Superconducting nanowires as quantum phase-slip junctions *Nat. Phys.* **2,** 169 (2006).
2. Mooij, J. E. *et al.* Superconductor-insulator transition in nanowires and nanowire arrays. *New J. Phys.* **17,** 033006 (2015).
3. Kawaguti, T. Shinozaki, B. & Fujimori, F. Superconducting transition of quench-condensed ultrathin films. *J. J. Appl. Phys.* Suppl. **26–3**, 1329 (1987).
4. Haviland, D. B. Lui, Y. & Goldman, A. M. Onset of superconductivity in the two-dimensional limit. *Phys. Rev. Lett.* **62,** 2180 (1989).
5. Finkel'stein, A. M. Suppression of superconductivity in homogeneously disordered systems. *Physica B* **197,** 636 (1994).
6. Ezaki, S. *et al.* Localization and interaction effects in ultrathin epitaxial NbN superconducting films. *J. Phys.: Cond. Mat.* **24,** 475702 (2012).
7. Oreg, Y. & Finkelstein, A. M. Suppression of Tc in superconducting amorphous wires. *Phys. Rev. Lett.* **83,** 191 (1999).
8. Goldman, A. M. Superconductor-insulator transitions. *Int. J. Mod. Phys. B* **24,** 4081 (2010).
9. Langer, J. S. & Ambegaokar, V. Intrinsic Resistive Transition in Narrow Superconducting *Channels. Phy. Rev*. **164,** 498 (1967).
10. McCumber, D. E. & Halperin, B. I. Time scale of intrinsic resistive fluctuations in thin Superconducting wires. *Phys. Rev.* **1,** 1054 (1970).

11. Giordano, N. Evidence for macroscopic quantum tunneling in one-dimensional superconductors. *Phys. Rev Lett.* **61,** 2137 (1988).
12. Bezrydin, A. Lau C. N. & Thinkham, M. Quantum suppression of superconductivity in ultrathin nanowires. *Nature (London)* **404,** 971 (2000).
13. Tinkham, M. & Lau, C. N. Quantum limit to phase coherence in thin superconducting wires. *Appl. Phys. Lett.* **80,** 2946 (2002).
14. Bollinger, A. T., Dinsmore III, R. C., Rogachev, A. & Bezryadin, A. Determination of the superconductor-insulator phase diagram for one-dimensional wires. *Phys. Rev. Lett.* **101,** 227003 (2008).
15. Altomare, F. *et al.* Evidence for Macroscopic quantum tunneling of phase slips in long one-dimensional superconducting Al wires. *Phys. Rev. Lett.* **97,** 017001 (2006).
16. Lehtinen, J. S. *et al.* Evidence of quantum phase slip effect in titanium nanowires. *Phys. Rev. B*, **85,** 094508 (2012).
17. Ning, W. *et al.* Superconductor–insulator transition in quasi-one-dimensional single-crystal Nb_2PdS_5 Nanowires. *Nano Lett.* **15,** 869 (2015).
18. Kim, H. Jamali, S. & Rogachev, A. Superconductor-insulator transition in long MoGe nanowires. *Phy. Rev. Lett*. **109,** 027002 (2012).
19. Markovic, N. Lau, C. N. & Tinkham, M. The limits of superconductivity in MoGe nanowires. *Physica C* **387,** 44 (2003).
20. Chakravarty, S. Quantum fluctuations in the tunneling between superconductors. *Phys. Rev. Lett.* **49,** 681 (1982).
21. Schmid, A. Diffusion and localization in a dissipative quantum system. *ibid*. **51,** 1506 (1983).
22. Bulgadaev, S. A. Phase diagram of a dissipative quantum system. *JETP Lett.* **39,** 315 (1984).
23. Refael, G., Demler, E. & Oreg, Y. Superconductor to normal-metal transition in finite-length nanowires: Phenomenological model. *Phys. Rev. B* **79,** 094524 (2009).
24. Lau, C. N. *et al.* Quantum phase slips in superconducting nanowires. *Phys. Rev. Lett.* **87,** 217003 (2001).
25. Makise, K. *et al.* Characterization of NbTiN thin films deposited on various substrates. *IEEE Tran. on Appl. Supercon*. **21,** 139 (2010).
26. Goldman, A. M. & Markovic, N. Superconductor-insulator transitions in the two-dimensional limit. *Phys. Today* **51(11),** 39 (1998).
27. Fisher, M. P. A. Quantum phase transitions in disordered two-dimensional superconductors. *Phys. Rev. Lett.* **65,** 923 (1990).
28. Paalanen, M. A. Hebard, A. F. & Ruel, R. R. Low-temperature insulating phases of uniformly disordered two-dimensional superconductors. *Phys. Rev. Lett.* **69,** 1604 (1992).
29. Tinkham, M. *Introduction to Superconductivity* (New York: McGraw–Hill) (1996).
30. Golubev, D. S. & Zaikin, A. D. Quantum tunneling of the order parameter in superconducting nanowires. *Phys. Rev. B* **64,** 014504 (2001).
31. Arutyunov, K. Y. Golubev D. S. & Zaikin, A. D. Superconductivity in one dimension. *Phys. Rep.* **464,** 1 (2008).
32. Delacour, C. Pannetier, B. Villegier, J. C. & Bouchiat, V. Quantum and thermal phase slips in superconducting niobium nitride (NbN) ultrathin crystalline nanowire: Application to single photon detection. *Nano Lett.* **12,** 3501 (2012).
33. Rogachev, A. Bollinger, A. T. & Bezryadin, A. Influence of high magnetic fields on the superconducting transition of one-dimensional Nb and MoGe nanowires. *Phy. Rev. Lett*. **94,** 017004 (2005).

Author Contributions

K.M. performed most of the experiments and analyzed the data. H.T. cotributed to the growth of nanowires. Y.T. and S.T. contributed to the experiments. All of the text of the paper was written jointly K.M. and B.S.

Additional Information

Competing financial interests: The authors declare no competing financial interests.

How to cite this article: Makise, K. *et al.* Duality picture of Superconductor-insulator transitions on Superconducting nanowire. *Sci. Rep.* **6**, 27001; doi: 10.1038/srep27001 (2016).